Electron loss from 1.4 MeV/u $U^{4,6,10+}$ ions colliding with Ne, N_2, and Ar targets

R.D. DuBois[1], A.C.F. Santos[2], Th. Stöhlker[3], F. Bosch[3], A. Bräuning-Demian[3], D. Banas[3], A. Gumberidze[3], S. Hagmann[3], C. Kozhuharov[3], R. Mann[3], A. Oršić Muthig[3], U. Spillmann[3], S. Tachenov[3], W. Bart[4], L. Dahl[4], B. Franzke[4], J. Glatz[4], L. Gröning[4], S. Richter[4], D. Wilms[4], K. Ullmann[4], and O. Jagutzki[5]

[1] University of Missouri-Rolla, Rolla, MO 65409, USA;

[2] Centro Federal de Educação Tecnológica de Química, Rio de Janerio, Brazil 26530-060

[3] Atomic Physics Division, GSI, 64291 Darmstadt, Germany;

[4] Accelerator Division, GSI, 64291 Darmstadt, Germany;

[5] Institut für Kernphysik der J.W. Goethe Universität Frankfurt,

August-Euler-Str. 6, Frankfurt am Main, Germany

EXT-2004-095
15/07/2004

Abstract:

Absolute, total, single, and multiple electron loss cross sections are measured for 1.4 MeV/u $U^{4,6,10+}$ ions colliding with neon and argon atoms and nitrogen molecules. It is found that the cross sections all have the same dependence on the number of electrons lost and that multiplying the cross sections by the initial number of electrons in the 6s, 6p, and 5f shells yields good agreement between the different projectiles. By combining the present data with previous measurements made at the same velocity, it is shown that the scaled cross sections slowly decrease in magnitude for incoming charge states between 1 and 10 whereas the cross sections for higher charge state ions fall off much more rapidly.

Introduction:

Energetic ion beams are routinely used to study fundamental atomic interactions such as excitation and ionization or to provide information about the structure of isolated atoms and molecules. Interactions with condensed phase materials have also been investigated by bombarding thin foils or solids with energetic ions. At very high energies, ion beams are used to study nuclear and subnuclear processes. Recently, very intense beams of high energy, heavy ions are being used or have been proposed for studying a) high energy density and plasma processes and b) nuclear processes and the structure of rare isotopes lying far off the nuclear stability curve. Intense beam studies require not only the ability to generate and accelerate intense ion beams to high energies, but perhaps also confining them in storage rings. Thus, minimizing detrimental effects such as loss of beam intensity and interactions with the vacuum walls and focusing elements and maximizing the beam energy density and storage lifetimes is essential.

Accomplishing this requires information about the absolute probabilities and resultant charge states when ion beams are ionized in interactions with residual gases present in accelerator beamlines or storage rings. Of particular interest is information about stripping of high energy, low-charge-state, heavy ions since these are the types of ions required for high energy density and intense beam studies. Although numerous experimental studies of projectile ionization were performed in the 1960's and 70's [1,2], little information pertaining to stripping of fast, low-charge-state, heavy ions exists. This is because heavy ion accelerators and switching magnets are not designed for low-charge-state ions.

During the past few years this problem has been addressed by measuring cross sections for electron loss from MeV/u heavy ions with charge states far below the equilibrium charge state. The emphasis of these studies has been to provide information about stripping probabilities and products, which can be used to extrapolate to the high energies and very low charge state beams of interest. For example, we recently reported [3] absolute cross sections for electron loss by 0.7 and 1.4 MeV/u $Ar^{1,2+}$ and Xe^{3+} ions. At the Texas A&M cyclotron, stripping of $Ar^{6,8+}$ [4], Kr^{7+} and Xe^{11+} [5], and Xe^{18+} [6,7] ions have been measured. On the theoretical side, calculations for electron loss from these multi-electron projectiles have been performed using the Born approximation [8-11] and the classical trajectory Monte Carlo method [6,7,12]. The major difference between the two theoretical methods is that the Born approximation scales single electron transitions and predicts an E^{-1} energy dependence at high energies whereas the CTMC method handles many electron transitions and predicts a slower dependence of $E^{-1/2}$.

The present work extends the information to extremely heavy, low-charge-state MeV/u ions, namely to 1.4 MeV/u $U^{4,6,10+}$ ions. Uranium ions were chosen for several reasons. First, they are ions of interest for future studies at GSI-Darmstadt. Second, in the US Heavy Ion Fusion Program, using very heavy low-charge-state beams such as Pb^{+} provides the maximum input power density that can be delivered to small DT (deuterium-tritium) pellets. Third, at 1.4 MeV/u data for stripping higher charge state uranium ions are available. Thus, a more complete picture of how the cross sections scale as a function of the initial charge state can be obtained.

Experimental procedure:

The experimental procedure was the same as we used in our previous study of stripping of low charge state argon and xenon ions [3]. Basically this consisted of using the GSI UNILAC to accelerate beams of uranium ions to 1.4 MeV/u. The beams were then passed through a stripping chamber after which the post collision components of the beam were separated with a magnetic field and detected using a two-dimensional position sensitive detector. Slits inserted at the entrance and exit of the stripping chamber were used to collimate and define the beam and also to provide differential pumping both upstream and downstream from the stripping chamber. Valving off the main pumps to the stripping chamber produced a pseudo static target between the two slits.

As was done in our previous study the absolute target density was calibrated by measuring the post collision charge state fractions of a 0.74 MeV/u He^{+} beam. These fractions were measured as a function of the pressure read near the periphery of the stripping chamber using an ion gauge. The measured charge state fractions were compared to values calculated as a function of target line density using known cross-sections (see ref. 3 for cross section references). From this comparison, calibration curves of absolute target line density versus target gas pressure were generated for each target gas. Because of the pseudo static target, the line density should be directly proportional to the measured pressure and when adjusted for gauge sensitivities and gas dependent pumping rates, all target gases should fall on a single curve.

In Fig. 1 we plot the line density versus the target gas pressure, P_{gas}, where $P_{gas} = (P - P_{bg})$*gas sensitivity. Here P is the pressure read with target gas present and P_{bg} is the background pressure, assumed to be predominantly N_2. For N_2, a sensitivity of 1 was used with the sensitivities for Ne and Ar being adjusted to yield a single curve of line density versus pressure. Results are shown in Fig. 1 along with the results from our previous study performed in 2002 where a slightly different procedure was used. Note the good agreement except for our previous neon calibration. This comparison implies that our results in reference 3 for a neon target are too small by roughly 30%. We note that renormalizing our previous neon target data by this amount would make them in almost perfect agreement with CTMC calculations (see Fig. 7 in ref. 3).

Returning to the present experiment, cross-sections measurements were obtained in the following fashion. A particular charge state uranium beam was accelerated to 1.4 MeV/u, the intensity was reduced and the beam was focused on the entrance aperture to the scattering chamber. The post collision magnetic field was adjusted such that the main beam and the electron loss components were positioned on a two-dimensional position sensitive detector. For U^{4+} four well-separated beam components could be detected. For U^{6+} and U^{10+} different magnetic fields and less separation between the various charge states were used and 7, 10, respectively, beam components were detected. Fast histograming electronics and a personal computer were used to record two-dimensional charge state information, which was converted to one-dimensional spectra as shown in Fig. 2. This process was repeated for five or six pressures ranging from a background pressure to pressures where approximately 30 percent of the main beam intensity was

lost. Note that in Fig. 2 the structure seen near channel zero is due to a higher background rate caused by localized damage to the detector. In the data analysis, effects from this increased background were minimized by a peak fitting routine mentioned below and/or integrating the two-dimensional spectra in a manner where it was possible to eliminate most of the extraneous signal in the damaged location.

By decreasing the beam intensity it was also demonstrated that no counting rate detection efficiency losses occurred. After data collection, charge state fractions were calculated from integrated peaks minus backgrounds. For U^{4+} the peaks were well separated and a simple summation was used for integration. For $U^{6,10+}$ the peaks were fitted by Gaussians and a linear background was subtracted. Uncertainties in peak intensities due to fitting procedures and background subtraction were generally estimated to be less than 5%. From the integrated intensities, charge state fractions were calculated then plotted as a function of target density using the density calibration described above. These growth curves were fitted with first and second-degree polynomials with the coefficient of the linear term being the cross-section. In our previous study, we then solved sets of coupled equations involving the charge state fractions in order to remove contributions from multiple collisions, which proved to be important in cases where many electrons were lost. This was not necessary in the present study because data were collected using lower target densities.

Results:

Absolute cross sections for total, single, and multiple electron loss by 1.4 MeV/u $U^{4,6,10+}$ ions in collisions with neon, argon, and molecular nitrogen targets are tabulated in Table I

and shown graphically in Fig. 3. The tabulated cross sections are in units of 10^{-16} cm^2 with the numbers in parenthesis the percent uncertainty in fitting the polynomial to the data. Fitting uncertainties less than 5% are not shown. Not included are uncertainties in calibrating the target density, which primarily come from uncertainties in the absolute cross sections used to calculate the charge state fractions. These are taken to be ±25%. Also not included are uncertainties in extracting the peak areas, which as stated above are less than 5%. Thus, the overall uncertainties in the absolute cross sections presented here range from roughly ±25 to 30%.

In Fig. 3 the cross sections have been scaled by $N_{eff}^{-0.4}$ where N_{eff} is the effective number of projectile electrons that are available for removal. This scaling was extracted by analyzing a large database of stripping cross sections for a wide variety of ions [13]. Although N_{eff} is a poorly defined quantity, it was found that for low charge state ions using the number of electrons contained in the outmost subshells provided the best results. For higher charge state ions, generally using the number of electron in the entire shell outside a rare gas core was more appropriate. In Fig. 3, the number of electrons in the 6s, 6p, and 5f shells of the incoming ion were used. As seen, for loss of up to six electrons this scaling works quite well. Also note that the curves for the various targets have been shifted for display purposes but all demonstrate the same dependence with respect to the number of electrons lost. For U^{10+} the average number of electrons lost per collision is found to be 3.4, independent of target gas. For U^{4+} and U^{6+} Fig. 3 implies that the average number of electrons lost would be very similar had more loss channels been measured. As a final note, the relative behavior as a function of target atomic number,

Z_T, under the assumption that an atomic nitrogen target can be simulated by ½ the molecular nitrogen value, agrees extremely well with the dependence found by Watson et al. [7] in their detailed study of electron loss by Xe^{18+} ions.

In Figures 4 and 5, our current data are combined with our previous 1.4 MeV/u measurements [3] and higher charge state data from Refs 14-16 in order to investigate how the cross sections for electron loss from medium and heavy ions (projectiles with nuclear charges, Z_P, larger than 18) depend on the incoming charge state. As seen, the total loss cross sections are only about 30% smaller for a 10+ ion than for a 1+ ion. In this same range, the single loss cross sections decrease by roughly a factor of two, the double loss cross sections more slowly, while the triple loss cross sections are nearly constant. Also, at least for the data available, medium and heavy projectiles all conform to the same curves. This is in sharp contrast to the behavior for higher charge state projectiles where for clarity we only show single loss cross sections. As seen, there is a strong dependence on the incoming charge state and clear distinctions for different projectiles. Identical behaviors are found for stripping by argon and nitrogen targets.

The lines in Figures 4 and 5 are simply to guide the eye. In addition, typical absolute uncertainties are indicated by the vertical lines on the single loss curve around $q_{in} = 4$. To avoid confusion, note that in Fig. 5 the cross sections are for atomic nitrogen obtained by dividing our molecular nitrogen cross sections by two. As a final comment, the only previous measurement available for direct comparison is for single, double, and triple loss in U^{10+} - N_2 collisions [16]. For clarity, those cross sections are plotted at a slightly

shifted charge of 10.5 in Fig. 5. The present measurements are nearly a factor of 2 smaller than those from Ref. 16. This discrepancy is disconcerting but rechecks confirmed that based on the input cross sections used, no errors were made in calibrating our N_2 target densities. In addition, the present cross sections systematically increase as a function of target atomic number, Z_T, as expected. Finally, if our present cross sections were a factor of two larger, figures 4 and 5 indicate that the scaled cross sections increase with increasing projectile charge up to charge state 10.

Summary:

To summarize, new experimental data have been presented for electron loss from 1.4 MeV/u low-charge-state uranium ions. Scaling the cross sections by the effective number of projectile electrons available for removal showed nearly identical features, independent of incoming charge state and target. The target dependence was found to be in good agreement with that reported by Watson et al. in a study which used Xe^{18+} data.

The present data complement and supplement existing data in the MeV/u range. Using the present and previously available information, the cross section dependence as a function of initial projectile charge state was investigated for projectile nuclear charges, Z_P, ranging from 18 to 92. It was found that for incoming charge states where $q_{in} < 0.1Z_P$ the cross sections decreased very slowly and data for different projectiles seemed to conform to the same curves. In contrast, for more highly stripped ions, $0.25Z_P < q_{in} < 0.60Z_P$, the cross sections decreased quite rapidly with increasing charge state and different behaviors for different Z_P projectiles are clearly observed.

Acknowledgements:

This work is supported by the U.S. Department of Energy, Grant No. ER54578. A.C.F. S. is grateful for support obtained from CNPq (Brazil) and for the opportunity to work at UMR.

References

1. H.H. Lo and W.L. Fite, Atomic Data **1**, 305 (1970).
2. R.C. Dehmel, H.K. Chau, and H.H. Fleischmann, Atomic Data **5**, 231 (1973).
3. R. D. DuBois, A. C. F. Santos, R. E. Olson, Th. Stöhlker, F. Bosch, A. Bräuning-Demian, A. Gumberidze, S. Hagmann, C. Kozhuharov, R. Mann, A. O. Muthig, U. Spillmann, S. Tachenov, W. Barth, L. Dahl, B. Franzke, J. Glatz, L. Gröning, S. Richter, D. Wilms, A. Krämer, K. Ullmann, and O. Jagutzki, Phys. Rev. A **68**, 042701 (2003).
4. D. Mueller, L. Grisham, I. Kaganovich, R.L. Watson, V. Horvat, K.E. Zaharakis and Y. Peng, Princeton Plasma Physics Laboratory Document PPPL-3713 (2002).
5. D. Mueller, L. Grisham, I. Kaganovich, R.L. Watson, V. Horvat, E. Zaharakis, M.S. Armel, Physics of Plasmas, **8**, 1753 (2001).
6. R.E. Olson, R.L. Watson, V. Horvat, and K.E. Zaharakis, J. Phys. B **35**, 1893 (2002).
7. R.L. Watson, Y. Peng, V. Horvat, G.J. Kim, and R.E. Olson, Phys. Rev. A **67**, 022706 (2003).
8. V.P. Shevelko, I.Yu. Tolstikhina and Th. Stöhlker, Nucl. Inst. And Meth. In Phys. Res. B **184**, 295 (2001).
9. V.P. Shevelko, D. Böhne and Th. Stöhlker, Nucl. Inst. And Meth. A **415**, 609 (1998).
10. V.P. Shevelko, O. Brînzanescu, W. Jacoby, M. Rau and Th. Stöhlker, Hyperfine Int. **114**, 289 (1998).
11. I.D. Kaganovich, E.A. Startsev, and R.C. Davidson, Phys. Rev. A **68**, 022707 (2003).
12. R.E. Olson, Nucl. Inst. and Meth. A **464,** 93 (2001).
13. A.C.F. Santos and R.D. DuBois, Phys. Rev. A **69**, 042709 (2004).

14. W. Erb and B. Franzke, GSI Report GSI-J-1-78, 119 (1978).

15. W. Erb, GSI Report GSI-P-7-78 (1978).

16. B. Franzke, IEEE Trans. on Nucl. Sci., NS-28, 2116 (1981).

Figures.

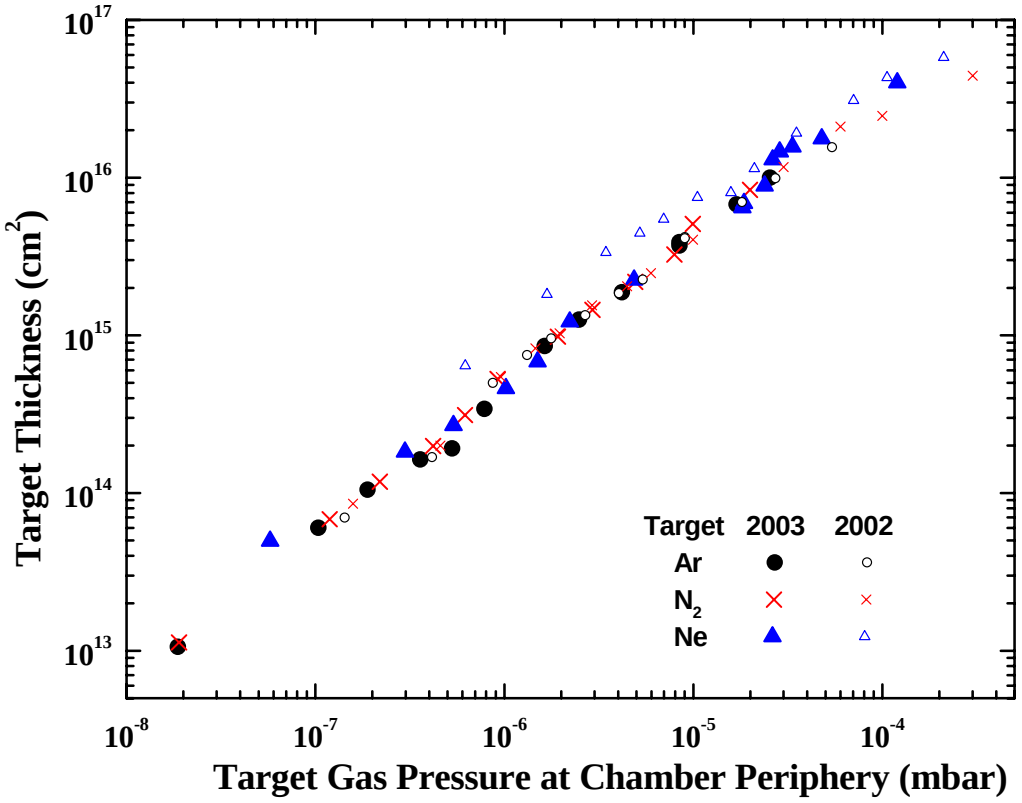

Figure 1. (Color online) Target thickness versus pressure of target gas near periphery of chamber. The thickness was determined from calculated and measured charge state fractions for 0.74 MeV/u He^+ impact. The target gas pressure was determined by subtracting the background pressure and multiplying by a gauge sensitivity. See text for details. Calibration data for the present work are compared to those from ref. 3.

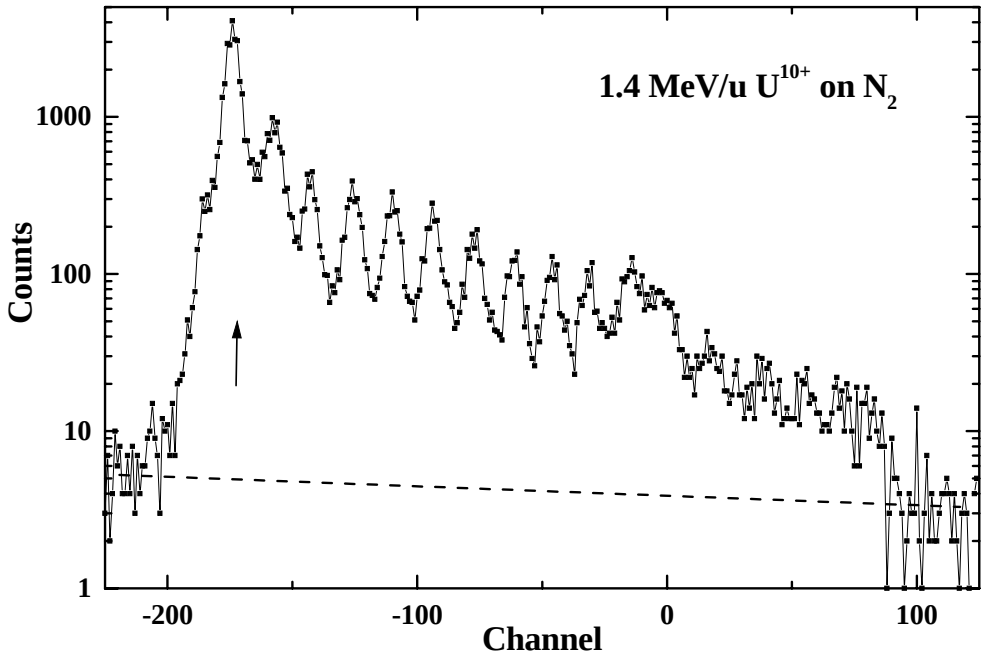

Figure 2. Projectile charge state spectrum for 1.4 MeV/u U^{10+} ions colliding with a molecular nitrogen target. The dashed line indicates a linear background which is subtracted in determining the charge state intensities. The arrow indicates charge state 10. The structure near channel zero is the result of localized damage to the detector.

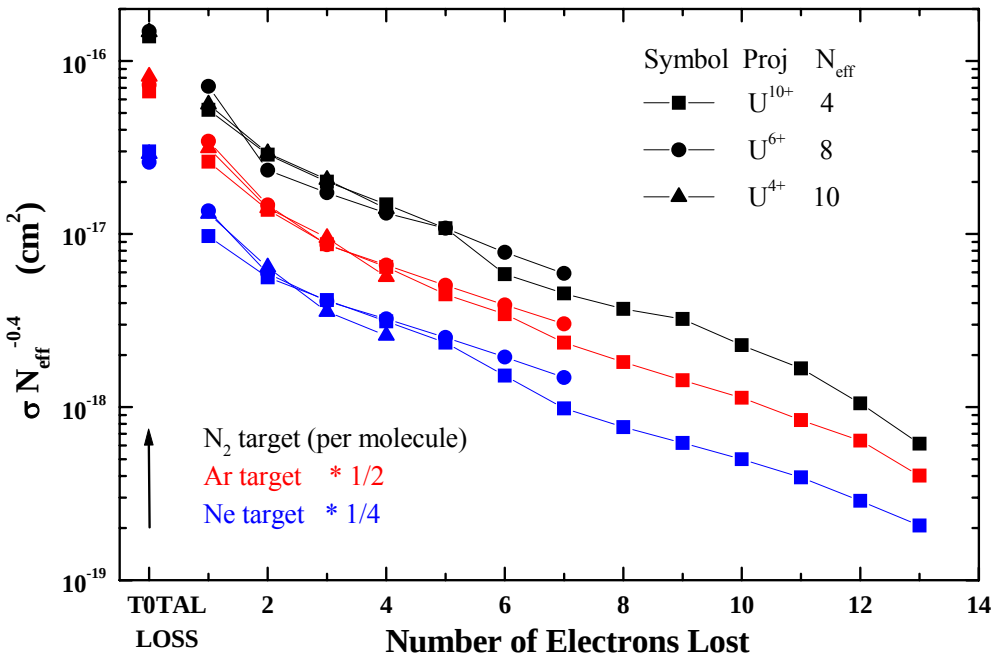

Figure 3. (Color online) Total, single, and multiple electron loss cross sections measured for 1.4 MeV/u $U^{4,6,10+}$ ions colliding with neon and argon atoms and nitrogen molecules. The cross sections have been scaled by N_{eff}, the total number of 6s, 6p and 5f electrons of the incoming ion. In this figure, the argon and neon data have been shifted downward for display purposes.

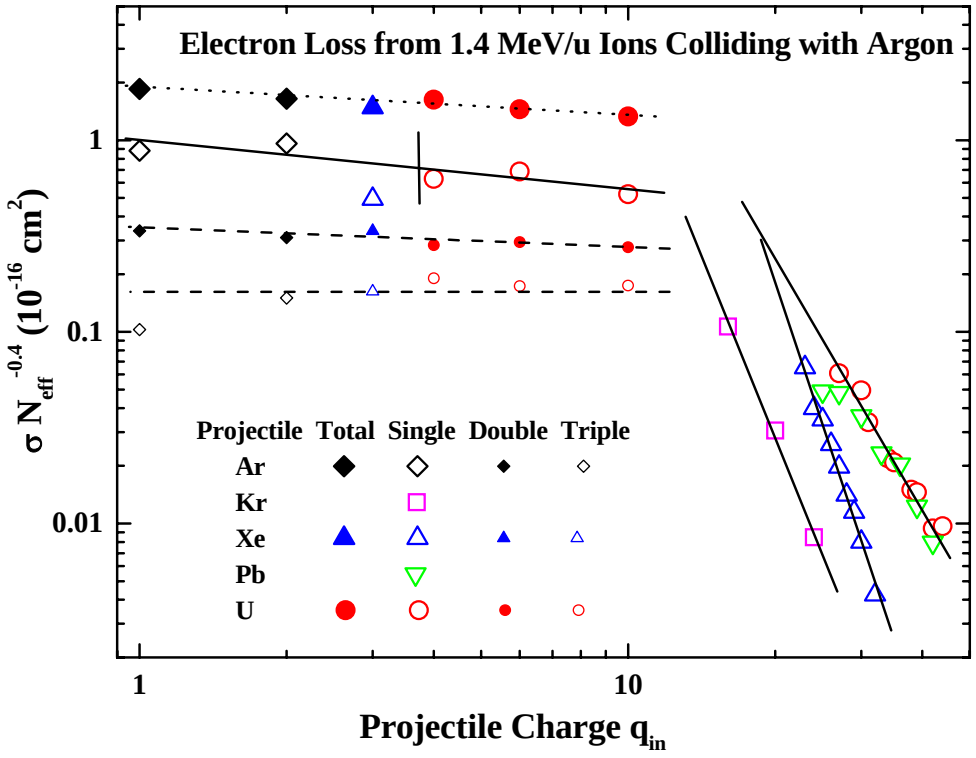

Figure 4. (Color online) Cross sections, as a function of incoming projectile charge state, for total, single, double, and triple electron loss from various 1.4 MeV/u ions colliding with argon. Data include the present measurements and cross sections taken from refs. 3,14,15. The cross sections have been scaled by the effective number of projectile electrons before the collision. See text for details. Lines are to guide the eye.

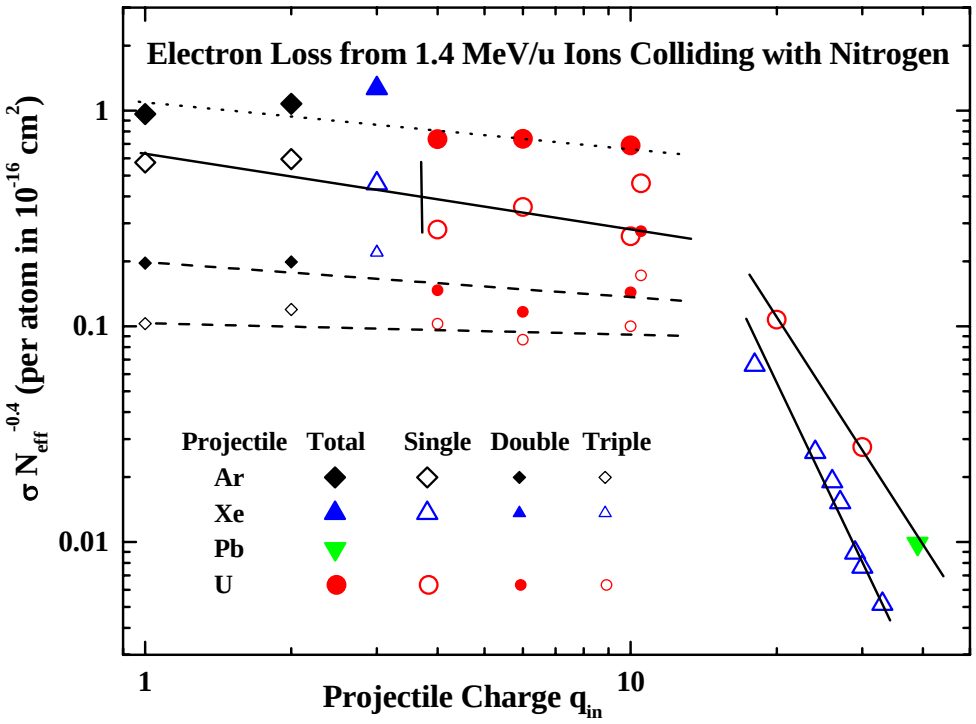

Figure 5. (Color online) Cross sections, per nitrogen atom, as a function of incoming projectile charge state, for total, single, double, and triple electron loss from various 1.4 MeV/u ions colliding with nitrogen. Data include the present measurements and cross sections taken from refs. 3,6,15,16. The cross sections have been scaled by the effective number of projectile electrons before the collision. See text for details. Lines are to guide the eye.

Table I. Cross sections per collision, in units of 10^{-16} cm^2, for total (all), single, and multiple electron loss from 1.4 MeV/u $U^{4,6,10+}$ ions colliding with neon and argon atoms and molecular nitrogen targets. The first two columns list the incoming and outgoing uranium charge states. The numbers in parenthesis give the percent uncertainties in extracting cross sections from growth curves for cases where the fitting uncertainties exceed 5%. Total uncertainties include these plus statistical uncertainties and uncertainties due to calibrating the target density. See text for details.

q_{in}	q_{out}	N_2	Neon	Argon
4	all	3.70 (5%)	2.92	4.09
4	5	1.41 (15%)	1.32	1.58
4	6	0.738 (18%)	0.645 (7%)	0.711 (11%)
4	7	0.517	0.358	0.478 (10%)
4	8	0.352	0.260	0.284 (8%)
4	9	0.170	0.127	0.125
4	10	0.0334 (21%)	0.0328 (5%)	0.0189 (9%)
6	all	3.41 (9%)	2.39	3.34 (6%)
6	7	1.64 (9%)	1.25 (6%)	1.58 (13%)
6	8	0.537	0.544 (6%)	0.676 (15%)
6	9	0.398	0.375 (6%)	0.398 (5%)
6	10	0.303	0.297 (7%)	0.304
6	11	0.248	0.232 (5%)	0.232 (5%)
6	12	0.180	0.179 (9%)	0.179
6	13	0.136	0.136 (8%)	0.139 (5%)
10	all	2.41	2.09	2.32
10	11	0.910 (10%)	0.677	0.911
10	12	0.500 (9%)	0.391	0.481
10	13	0.349 (9%)	0.289	0.304 (6%)
10	14	0.258 (12%)	0.218	0.225
10	15	0.188 (8%)	0.164	0.156 (5%)
10	16	0.102	0.106	0.120 (5%)
10	17	0.0789	0.0684	0.0821
10	18	0.0642	0.0533	0.0634

10	19	0.0562	0.0432	0.0497
10	20	0.0397	0.0348	0.0394 (5%)
10	21	0.0291	0.0273	0.0293
10	22	0.0183	0.0200	0.0223
10	23	0.0107	0.0144	0.0140